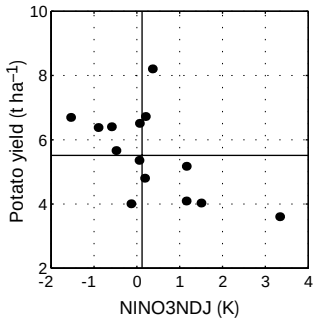

Figure 4 Central Andean harvests and El Niño. Shown are potato yields (in tonnes per hectare) for Puno department plotted against NINO3NDJ, 1980–81 to 1993–94. The solid lines represent median values for each axis.

Given the sensitivity of potatoes to drought, this reduction in precipitation may account for part of the relationship between June high-cloud amount and potato harvests (Fig. 1a). A more complete analysis of the effect of climate on crops must include other climatic variables, most notably temperature. In fact, we find a strong monotonic relationship between ENSO and mean monthly temperatures in the central Andes region, with warmer mean temperatures in the central Andes during El Niño years. Though the effect of temperature on crop growth is not obvious, the consequence of ENSO for potato yields is convincingly demonstrated from preliminary analysis of potato-yield data from Puno department near Lake Titicaca (Fig. 4). Significant reductions in potato yield are observed for warm ENSO years. A 2-bin χ^2 test shows significance at the 90% level. The linear correlation value is −0.6. □

Received 22 March; accepted 11 November 1999.

1. Zimmerer, K. S. *Changing Fortunes: Biodiversity and Peasant Livelihood in the Peruvian Andes* (Univ. California Press, Berkeley, 1996).
2. Salomon, F. & Urioste, G. L. *The Huarochiri Manuscript: A Testament of Ancient and Colonial Andean Religion* (Univ. Texas Press, Austin, 1991 [c. 1608]).
3. Ballón Aguirre, E., Cerrón Palomino, R. O. & Chambi Apaza, E. *Vocabulario Razonado de la Actividad Agraria Andina. Terminología Agraria Quechua.* (Centro de Estudios Regionales Andinos "Bartolomé de Las Casas", Cusco, 1992).
4. Urton, G. *At the Crossroads of the Earth and The Sky: An Andean Cosmology* (Univ. Texas Press, Austin, 1981).
5. Grillo Fernández, E., Quiso Choque, V., Rengifo Vásquez, G. & Valladolid Rivera, J. *Crianza Andina de la Chacra* (Proyecto Andino de Tecnología Campesina, Lima, 1994).
6. Mishkin, B. Cosmological ideas among the Indians of the southern Andes. *J. Am. Folklore* **53,** 225–241 (1940).
7. Morote Best, E. La fiesta de San Juan, el Bautista. *Arch. Peruanos Folklore* **1,** 160–200 (1953).
8. Orlove, B. S. Two rituals and three hypotheses: an examination of solstice divination in southern highland Peru. *Anthropol. Quart.* **52,** 86–98 (1979).
9. Lira, J. A. *Farmacopea Tradicional Indígena y Prácticas Rituales* (El Condor, Lima, 1946).
10. Camino, A., Recharte, J. & Bidegaray, P. *La Tecnología en el Mundo Andino. Runakunap Kawsayninkupaq Rurasqankunaqa* Vol. 1 (eds Lechtman, H. & Soldi, A. M.) 261–281 (Universidad Nacional Autónoma de México, Mexico City, 1981).
11. Goland, C. *Cultivating Diversity: Field Scattering as Agricultural Risk Management in Cuyo Cuyo, Dept. of Puno, Peru* (Working Paper No. 4, Research Project on Production, Storage and Exchange in a Terraced Environment on the Eastern Andean Escarpment, Department of Anthropology, Univ. North Carolina, Chapel Hill, 1992).
12. Kolata, A. *Valley of the Spirits: A Journey into the Lost Realm of the Aymara* (Wiley, New York, 1996).
13. Carter, W. E. & Mamani, M. *Irpa Chico: Individuo y Comunidad en la Cultura Aymara* (Juventud, La Paz, 1982).
14. Mamani, M. in *Raíces de América: el Mundo Aymara* (ed. Albó, X.) 75–131 (Alianza, Madrid, 1988).
15. Yampara Huarachi, S. in *La Cosmovisión Aymara* (eds van den Berg, H. & Schiffers, N.) 143–186 (UCB/HISBOL, La Paz, 1992).
16. Kraft, K. E. *Andean Fields and Fallow Pastures: Communal Land Use Management under Pressures for Intensification*. Thesis, Univ. Florida (1995).
17. Beukema, H. P. & van de Zaag, D. E. *Introduction to Potato Production* (Pudoc, Wageningen, 1990).
18. MacKerron, D. K. L. & Jeffries, R. A. The distribution of tuber sizes in droughted and irrigated crops of potato. I. Observations on the effect of water stress on graded yields from differing cultivars. *Potato Res.* **31,** 269–278 (1988).
19. Bauer, B. S. & Dearborn, D. S. P. *Astronomy and Empire in the Ancient Andes: The Cultural Origins of Inca Sky Watching*. (Univ. Texas Press, Austin, 1995).
20. de Arriaga, P. J. *The Extirpation of Idolatry in Peru* (Univ. Kentucky Press, Lexington, 1968 [1621]).
21. Anonymous Jesuit priest Misión de las provincias de los Huachos y Yauyos. *Rev. Histórica* (Lima) **6,** 180–197 (1919).
22. de Santillán, F., Valera, B. & Pachacuti, J. de S. C. *Tres Relaciones de Antigüedades Peruanas* (Guarania, Asunción, 1950).
23. Rossow, W. B. & Schiffer, R. A. ISCCP cloud data products. *Bull. Am. Meteorol. Soc.* **72,** 2–20 (1991).
24. Kent, G. S. *et al.* Surface temperature related variations in tropical cirrus cloud as measured by SAGE II. *J. Clim.* **8,** 2577–2594 (1995).
25. Liao, X., Rossow, W. B. & Rind, D. Comparison between SAGE II and ISCCP high-level clouds 1. Global and zonal mean cloud amounts. *J. Geophys. Res.* **100,** 1121–1135 (1995).
26. Kalnay, E. *et al.* The NCEP/NCAR 40 year reanalysis project. *Bull. Am. Meteorol. Soc.* **77,** 437–471 (1996).
27. Schaefer, B. E. Astronomy and the limits of vision. *Vistas Astron.* **36,** 311–361 (1993).
28. Thompson, L. G., Mosley-Thompson, E. & Arnao, B. J. El Niño-Southern Oscillation events recorded in the stratigraphy of the tropical Quelccaya ice cap, Peru. *Science* **226,** 50–53 (1984).
29. Aceituno, P. On the functioning of the Southern Oscillation in the South American sector. Part I: Surface climate. *Mon. Weath. Rev.* **116,** 505–524 (1988).
30. Frisancho, A. R. *et al.* Developmental, genetic and environmental components of aerobic capacity at high altitude. *Am. J. Phys. Anthropol.* **96,** 431–442 (1995).

Supplementary information is available on *Nature*'s World-Wide Web site (http://www.nature.com) or as paper copy from the London editorial office of *Nature*.

Acknowledgements

We thank G. Urton for insights into Andean ethnoastronomy, G. Rasmussen for discussions on visibility and cirrus cloud, G. Scott for providing potato yield data for Puno department, Peru, and R. Bishop, K. Cook, D. Dearborn, D. Helfand, A. Kaplan, G. Kiladis, J. Lenters, M. Sarazin and B. Schafer for comments. M.A.C. thanks B. D'Achille for first making him aware of the Andean forecasting scheme.

Correspondence and requests for materials should be addressed to B.S.O. (e-mail: bsorlove@ucdavis.edu).

Channelized fluid flow in oceanic crust reconciles heat-flow and permeability data

A. T. Fisher* & K. Becker†

** Earth Sciences Department, University of California, Santa Cruz, California 95064, USA*
† Division of Marine Geology and Geophysics, Rosenstiel School of Marine and Atmospheric Sciences, University of Miami, Miami, Florida 33145, USA

Hydrothermal fluid circulation within the sea floor profoundly influences the physical, chemical and biological state of the crust and the oceans. Circulation within ridge flanks (in crust more than 1 Myr old) results in greater heat loss[1–3] and fluid flux[4] than that at ridge crests and persists for millions of years, thereby altering the composition of the crust and overlying ocean[5,6]. Fluid flow in oceanic crust is, however, limited by the extent and nature of the rock's permeability[7]. Here we demonstrate that the global data set of borehole permeability measurements in uppermost oceanic crust[7–9] defines a trend with age that is consistent with changes in seismic velocity[10,11]. This trend—which indicates that fluid flow should be greatly reduced in crust older than a few million years—would appear to be inconsistent with heat-flow observations, which on average indicate significant advective heat loss in crust up to 65 Myr old[3]. But our calculations, based on a lateral flow model, suggest that regional-scale permeabilities are much higher than have been measured in boreholes. These results can be reconciled if most of the fluid flow in the upper crust is channelized through a small volume of rock, influencing the geometry of convection and the nature of fluid–rock interaction.

Permeabilities have been measured in oceanic crustal boreholes using a drill-string packer, a device that hydraulically seals a borehole so that fluid can be pumped into the formation and transient changes in pressure can be monitored[7]. These measurements yield "bulk" permeabilities close to the borehole, assumed to be distributed evenly within the isolated interval. Other methods, including interpretation of temperature logs within upper basement[12,13], and modelling of subseafloor tidal response recorded by pressures in

long-term sealed observatories[14], yield permeability estimates at larger scales. Until recently, borehole measurements were restricted to crustal ages ⩾6 Myr and did not indicate any permeability evolution trend; instead, these data suggested a narrow range for uppermost oceanic basement, 10^{-13} to 10^{-14} m^2 (ref. 7).

New borehole measurements in 0.9–3.6 Myr-old crust on the eastern flank of Juan of Fuca ridge[8], in combination with measurements made elsewhere[7,9], reveal a remarkably consistent trend in permeability evolution within uppermost basaltic basement (Fig. 1). Bulk permeability decreases rapidly as young crust ages, from about 10^{-10} m^2 to 10^{-13} m^2 over the first 3–4 Myr (Fig. 1a and b).

Recent compilations and surveys of seismic velocities in uppermost oceanic crust[10,11] show a similar trend: velocity increases rapidly during the first few million years, then more slowly during later times (Fig. 1c and d). Density calculations from near-bottom gravity measurements[15] also show a rapid increase in the first 1 Myr, but wireline logs in older boreholes suggest only small additional increases with age. Thus physical properties measurements are consistent with initially rapid pore infilling by mechanical and magmatic processes during the earliest stages of crustal evolution, and by slower diagenetic processes as ageing continues[16,17].

Global heat flow compilations[3] appear to conflict with this rapid-ageing model because they suggest that advective heat loss continues on average out to 65 Myr (Fig. 1e and f), despite the early permeability reduction. Regional heat-flow surveys indicate continued circulation in basement to even greater ages[18,19]. The global heat-flow data also show little dependence on sediment thickness, suggesting that a process other than sediment thickening may limit advective heat loss from the crust[3]. Here we suggest a model by which the physical properties and heat-flow data sets can be reconciled, based on lateral fluid fluxes required by the heat-flow data, calculations of fluid driving forces, and inferences regarding crustal heterogeneity.

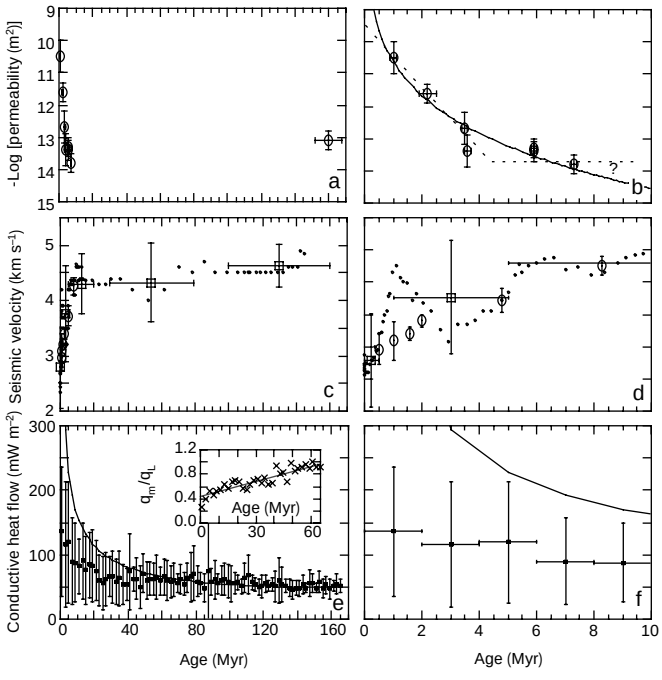

Figure 1 Bulk properties within uppermost oceanic crust, and heat loss versus crustal age. **a**, Permeability for 0–165 Myr (refs 7, 8). Horizontal and vertical bars indicate estimated uncertainties in crustal age and bulk permeability. **b**, Permeability for 0–10 Myr. Curves are least-squares best-fit exponential (solid) and straight-line segments fitted by eye (dashed). The ? indicates that the trend beyond 6–7 Myr is not constrained by observations. **c**, Seismic velocity for 0–165 Myr. Dots are medians of a moving 9-point window of a global data set[10]; squares are means, and 1 s.d. (vertical bars) and range of interval (horizontal bars) are also shown for same data; open circles are results from the flank of the East Pacific Rise[11], with 1 s.d. (vertical bars). **d**, Seismic velocity for 0–10 Myr. **e**, Oceanic heat flow and predicted values (GDH1[3]) based on crustal age, using 2-Myr bins (horizontal bars) and showing 1 s.d. within each bin (vertical bars). Inset, heat-flow suppression as a function of crustal age, with a least-squares best-fit line of $q_m/q_L = 0.43 + 0.0085 \times$ age (age in Myr). **f**, Sea-floor heat flow versus age for 0–10 Myr.

We assume that the global heat-flow data set reliably indicates advective heat loss from the crust (Fig. 1e, inset), and that hydrothermal circulation locally homogenizes temperatures in uppermost basement. Cold sea water enters this "well-mixed aquifer" and warms while flowing laterally until discharged at the sea floor[20] (Fig. 2a). Heat flow through sediments is mainly conductive, as vertical fluid flow is greatly restricted once the sediments are a few tens of metres thick. Net lateral fluid flow is the critical geometry for widespread heat removal from basement, because local convection will only redistribute heat, and vertical flow is inefficient at extracting heat over long horizontal distances. Vigorous flow in the uppermost crust is consistent with the global permeability data set[7,8] and with evidence for high water/rock ratios during alteration[5,21].

Heat is 'mined' by laterally flowing fluid, with heat flow suppression (q_m/q_L, where q_m is measured heat flow and q_L is lithospheric heat flow) dependent on sediment thickness and the basement layer thickness in which lateral flow occurs (h_s and h_b, respectively), sediment thermal conductivity (λ_s), the density and specific heat of water (ρ and c, respectively), distance from the fluid entry point (Δx), and the specific discharge of fluid in basement (Q_0, the volume flux per cross-sectional area)[20]:

$$\frac{q_m}{q_L} = \left[1 - \exp\left(\frac{-\lambda_s \Delta x}{Q_0 h_s h_b \rho c}\right)\right] \quad (1)$$

Sea-floor heat flow suppression as a function of age is known (Fig. 1e, inset), and we estimate sediment thickness based on crustal age and sedimentation rate, let Δx vary with crustal age, and calculate Q_0.

The driving forces moving fluid laterally through the crust can be linked to equation (1) using a form of Darcy's law:

$$Q_0 = -\frac{k}{\mu}\frac{dP}{dx} \quad (2)$$

Here μ is fluid viscosity, P is pressure, and k is formation permeability. In contrast to the situation at the ridge crests, there is only one significant source of lateral pressure gradients within ridge flanks: the difference between cooler and warmer columns of fluid entering and leaving the crust. The greatest difference in fluid pressure would arise from a connection between a cool recharge zone, in which bottom sea water moves rapidly into the crust, and a warm discharge zone, in which heated hydrothermal water rises adiabatically into the overlying ocean.

Combining equations (1) and (2) allows calculation of the formation permeability of upper oceanic crust required to allow sufficient lateral flow so as to explain the observed heat-flow suppression. We include a temperature dependence in fluid viscosity and density, and assume that the mean distance between fluid entry and exit points increases with time, because faults and basement outcrops that extend to the sea floor are likely to become more widely spaced with age as sediment thickens. dP/dx is calculated from the difference in fluid density between downflow and upflow zones, and by letting $dx = 5.0 + 0.5 \times$ age (in km and Myr, respectively), which yields distances between upflow and downflow zones of 5.0–37.5 km over ages of 1–65 Myr. We let Δx, the characteristic lateral flow length, be one half the downflow–upflow spacing, consistent with apparent scales of flow in several settings[20,22–24]. The temperature assumed for the fluid within upflow zones is that at the sediment–basement interface, with lithospheric heat flow based on crustal age, and the pressure difference between downflow and upflow zones is calculated as

$dP \approx \Delta\rho g(h_s + h_b)$. Because there are practical limits on the available driving forces (described below), and because crustal permeability varies by many orders of magnitude, these calculations are robust to reasonable modifications to the stated assumptions.

The maximum driving forces available for lateral fluid flow within young ridge flanks (1–5 Myr) are a few kilopascals within crust having a thin sediment layer, to several hundred kilopascals if the sediment layer is thicker (Fig. 2b), because permeable basement is deeper and hotter. Pressure differences increase more rapidly with age within crust experiencing higher sedimentation rates. We calculate higher pressure differences for young crust if we use the temperature at the base of the permeable layer to calculate the upflow temperature, but these pressure differences decrease with time because the effect of a rapid decline in lithospheric heat input initially overwhelms the effect of increasing sediment thickness. The lateral specific discharge required to suppress sea-floor heat flow decreases as the crust ages (Fig. 2c), because a deeper hydrothermal layer is hotter and can mine heat more efficiently, and because the thermal anomaly decreases with age (Fig. 1e and f). For young ridge flanks, these calculations indicate specific discharge of the order of 10^{-8} to 10^{-6} m s^{-1} (0.3–30 m yr^{-1}), consistent with other models[20,22,24] and with ^{14}C age estimates for crustal fluids[25].

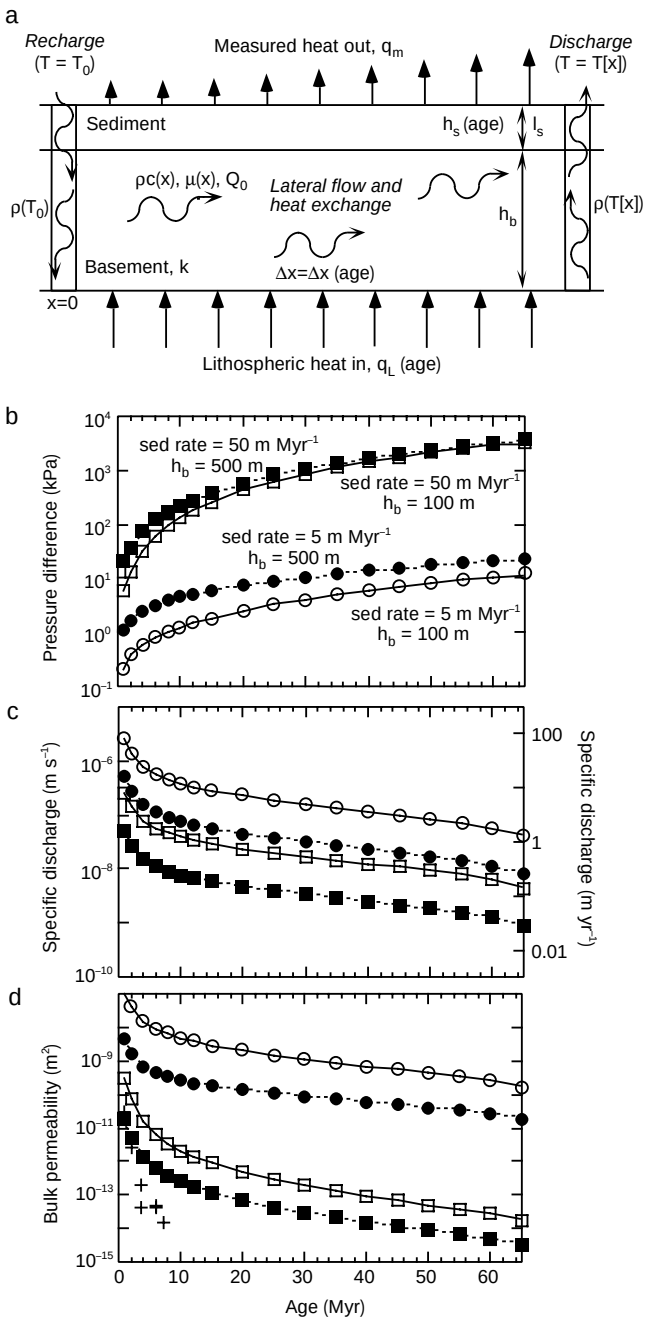

Figure 2 Conceptual model and calculations for lateral fluid flow through upper oceanic crust. **a**, Diagram of the ''well-mixed aquifer'' model (modified from ref. 20). Symbols defined in text. Some parameters are labelled on plots; other values are: $\lambda_s = 1.2\,W\,m^{-1}\,K^{-1}$, $T_0 = 0\,°C$, $c = 4{,}200\,J\,kg^{-1}\,K^{-1}$, ρ and μ are calculated using the mean temperature along the flow path, h_s and Δx vary with crustal age (as described in text). **b**, Calculated pressure difference between recharge and discharge locations, assuming adiabatic vertical flow. Crustal parameters as labelled. **c**, Specific discharge (volume flux per area) for crustal parameters as in Fig. 1b, based on the linear fit to global heat-flow data (Fig. 1e, inset). **d**, Apparent bulk permeability for crustal parameters as in Fig. 1b, required by the observed heat-flow suppression (Fig. 1e), and necessary to allow the calculated specific discharge, given the largest available pressure gradient. Borehole permeability values plotted for reference (crosses).

The calculated formation-scale permeabilities vary with sediment thickness and flow depth, and the lowest permeabilities correspond to the greatest available pressure differences (Fig. 2d). Calculated permeabilities decrease with crustal age, but overlap borehole observations only for very young crust (≤2 Myr) having a thick permeable layer (500 m) and a high sedimentation rate (50 m Myr^{-1}) (Fig. 2d). None of the calculated permeability evolution curves include the abrupt decrease with age apparent in the borehole data for young crust, and calculations based on more typical abyssal sedimentation rates (5 m Myr^{-1}) are offset from observations by several orders of magnitude (Fig. 2d). The lowest calculated permeabilities (10^{-14} to 10^{-13} m^2 at 50–65 Myr) correspond to the largest available driving forces (1.0–3.0 MPa), which would be greater than lithostatic overburden unless sediment is very thick. Recent measurements from ridge-flank borehole observatories[26] indicate more modest differences in crustal fluid pressures, a few to several tens of kilopascals, as do estimates of flow rates from open hole temperature logs[13].

Matching the observed borehole permeability evolution trend would require a combination of deepening or thickening of the hydrothermal layer with age, or upflow and downflow zones that move closer together, which seems unlikely. We offer an alternative explanation. The bulk properties of upper oceanic crust (seismic, density and permeability) are correct as measured. Very young crust is fractured and open, seismic velocities are low, and bulk permeability is high. Within a few million years after leaving the ridge axis, much of the crustal porosity is lost, density and seismic velocity increase, and bulk permeability decreases. Large-scale hydrothermal circulation responsible for the documented thermal anomalies continues within discrete channels, spatially restricted regions that occupy a small volume of the crust. This concept is analogous to flow channelling within fractures and fault planes, a process known to control solute transport and water–rock interaction within fractured aquifers at a smaller scale[27]. In the upper oceanic crust, the extrusive section would contain the primary 'flow plane', with flow occurring preferentially through a network of connected channels such as breccia zones and pillow and flow boundaries. These channels would take the longest to infill, but they would have little effect on seismic velocities or density if they are metres or tens of metres apart and occupy a small crustal volume. Because thermal conduction is efficient, sea-floor heat-flow suppression would be indistinguishable from that resulting from ubiquitous flow within a more homogeneous upper basement.

Outcrops and high-angle normal faults would be critical to this channelized flow system, allowing fluids to penetrate through lower-permeability sediments and basement. The driving forces for large-scale flow could remain modest (Fig. 2b), as large-scale permeabilities would be high, and the flow channels would remain open until the crust is old because of their chemical isolation. At an average age of 65 Myr, continuing diagenesis, lower lithospheric heat flow, and increased spacing between outcrops and sediment-

penetrating faults would make lateral fluid flow within upper basement inefficient at removing heat. Circulation would continue within basement locally, redistributing heat or being thermally masked below thick sediments, but heat loss from the crust would be entirely conductive.

This model explains how free convection could be prevented despite very high effective permeabilities, enhancing the efficiency of lateral flow for advecting heat. It does not preclude local thermal homogenization of upper basement[28], either by organized or chaotic flow[29], but local convection could also be channelized. Unlike a homogeneous permeability model for the upper crust, our model is consistent with observed lithostratigraphic, hydrologic, and alteration heterogeneity[5,7,17,30]. There would still be chemically and biologically significant fluid flow within much of the upper crust, but fluid fluxes away from the primary channels would be small relative to those in the channels.

Some important implications for hydrogeology and fluid–rock interaction within oceanic ridge flanks follow from our model. First, most of the fluid flow within the uppermost oceanic crust of ridge flanks would be very strongly guided (perhaps fully constrained) by the permeability distribution. There would be no tendency for hydrothermal convection cells to form with any particular geometry, and flow channelling would reduce the tendency for small-scale convection cells to form, since crustal permeability would be both heterogeneous and highly anisotropic. Second, flow would be much less chaotic than in a homogeneous, isotropic porous system having the same formation-scale permeability. Local flow paths would be strongly influenced by crustal constructional, tectonic and alteration patterns. Third, water–rock ratios would be highly variable over small spatial distances, depending on proximity to primary flow channels, and reaction in surrounding rock would be limited by slower advection and diffusion away from the channels. Borehole permeability estimates from packer testing would indicate the bulk hydrologic properties of most of the upper crust—with decreasing permeability associated with infilling of pores and increasing seismic velocities in young crust—but the flow channels responsible for the ridge–flank heat-flow deficit (Fig. 1e), being spatially rare, would generally not be penetrated by vertical boreholes[8].

Testing of the model we report here can be performed by continuing to map out bulk permeability, apparent water age, and the distribution of lateral and vertical pressure gradients within oceanic crust, over a range of crustal ages. Understanding will also come from measuring permeability at a variety of lateral scales using the same boreholes and the same measurement methods, and by cross-hole testing, in order to establish the spatial dependence of properties. Coupled heat and fluid flow models will continue to provide insight, but should include heterogeneous permeability distributions and anisotropy. □

Received 18 May; accepted 11 November 1999.

1. Sclater, J. G., Jaupart, C. & Galson, D. The heat flow through oceanic and continental crust and the heat loss of the earth. *Rev. Geophys. Space Phys.* **18,** 269–311 (1980).
2. Stein, C. & Stein, S. A model for the global variation in oceanic depth and heat flow with lithospheric age. *Nature* **359,** 123–129 (1992).
3. Stein, C. & Stein, S. Constraints on hydrothermal heat flux through the oceanic lithosphere from global heat flow. *J. Geophys. Res.* **99,** 3081–3095 (1994).
4. Mottl, M. J. & Wheat, C. G. Hydrothermal circulation through mid-ocean ridge flanks: fluxes of heat and magnesium. *Geochim. Cosmochim. Acta* **58,** 2225–2237 (1994).
5. Alt, J. C. in *Seafloor Hydrothermal Systems: Physical, Chemical, Biological and Geological Interactions* (eds Humphris, S. E., Zierenberg, R. A., Mullineaux, L. S. & Thompson, R. E.) 85–114 (American Geophysical Union, Washington DC, 1995).
6. Elderfield, H. & Schultz, A. Mid-ocean ridge hydrothermal fluxes and the chemical composition of the ocean. *Annu. Rev. Earth Planet. Sci.* **24,** 191–224 (1996).
7. Fisher, A. T. Permeability within basaltic oceanic crust. *Rev. Geophys.* **36,** 143–182 (1998).
8. Becker, K. & Fisher, A. T. Permeability of upper oceanic basement on the eastern flank of the Endeavor Ridge determined with drill-string packer measurements. *J. Geophys. Res.* (in the press).
9. Bruns, T. & Lavoie, D. Bulk permeability of young backarc basalt in the Lau Basin from a downhole packer experiment (Hole 839B). *Proc. ODP Sci. Res.* **135,** 805–816 (1994).
10. Carlson, R. L. Seismic velocities in the uppermost oceanic crust: age dependence and the fate of layer 2A. *J. Geophys. Res.* **103,** 7069–7077 (1998).
11. Grevemeyer, I., Norbert, K., Villinger, H. & Weigel, W. Hydrothermal activity and the evolution of the seismic properties of upper oceanic crust. *J. Geophys. Res.* **104,** 5069–5079 (1999).
12. Becker, K., Langseth, M., Von Herzen, R. P. & Anderson, R. Deep crustal geothermal measurements, Hole 504B, Costa Rica Rift. *J. Geophys. Res.* **88,** 3447–3457 (1983).
13. Fisher, A. T., Becker, K. & Davis, E. E. The permeability of young oceanic crust east of Juan de Fuca Ridge determined using borehole thermal measurements. *Geophys. Res. Lett.* **24,** 1311–1314 (1997).
14. Wang, K. & Davis, E. E. Theory for the propagation of tidally induced pore pressure variations in layered subseafloor formations. *J. Geophys. Res.* **101,** 11483–411495 (1996).
15. Holmes, M. L. & Johnson, H. P. Upper crustal densities derived from seafloor gravity measurements: northern Juan de Fuca Ridge. *Geophys. Res. Lett.* **17,** 1871–1874 (1993).
16. Jacobson, R. S. Impact of crustal evolution on changes of the seismic properties of the uppermost oceanic crust. *Rev. Geophys.* **30,** 23–42 (1992).
17. Gillis, K. M. & Sapp, K. Distribution of porosity in a section of upper oceanic crust exposed in the troodos ophiolite. *J. Geophys. Res.* **102,** 10133–10149 (1997).
18. Embley, R., Hobart, M., Anderson, R. & Abbott, D. Anomalous heat flow in the northwest Atlantic, a case for continued hydrothermal circulation in 80 MY crust. *J. Geophys. Res.* **88,** 1067–1074 (1983).
19. Noel, M. & Hounslow, M. W. Heat flow evidence for hydrothermal convection in Cretaceous crust of the Madeira Abyssal Plain. *Earth. Planet. Sci. Lett.* **90,** 77–86 (1988).
20. Langseth, M. G. & Herman, B. Heat transfer in the oceanic crust of the Brazil Basin. *J. Geophys. Res.* **86,** 10805–10819 (1981).
21. Gillis, K. & Robinson, P. T. Distribution of alteration zones in the upper oceanic crust. *Geology* **16,** 262–266 (1988).
22. Baker, P., Stout, P., Kastner, M. & Elderfield, H. Large-scale lateral advection of seawater through oceanic crust in the central equatorial Pacific. *Earth. Planet. Sci. Lett.* **105,** 522–533 (1991).
23. Langseth, M. G., Becker, K., Von Herzen, R. P. & Schultheiss, P. Heat and fluid flux through sediment on the western flank of the Mid-Atlantic Ridge: a hydrogeological study of North Pond. *Geophys. Res. Lett.* **19,** 517–520 (1992).
24. Davis, E. E. *et al.* Regional heat-flow variations across the sedimented Juan de Fuca Ridge eastern flank: constrains on lithospheric cooling and lateral hydrothermal heat transport. *J. Geophys. Res.* **104,** 17675–17688 (1999).
25. Elderfield, H., Wheat, C. G., Mottl, M. J., Monnin, C. & Spiro, B. Fluid and geochemical transport through oceanic crust: a transect across the eastern flank of the Juan de Fuca Ridge. *Earth. Planet. Sci. Lett.* **172,** 151–165 (1999).
26. Davis, E. & Becker, K. Borehole observations record driving forces for hydrothermal circulation in young oceanic crust. *Eos* **79,** 369,F377–378 (1998).
27. Tsang, C. F. & Neretnieks, I. Flow channeling in heterogeneous fractured rocks. *Rev. Geophys.* **36,** 275–298 (1998).
28. Davis, E. E., Chapman, D. S., Forster, C. & Villinger, H. Heat-flow variations correlated with buried basement topography on the Juan de Fuca Ridge flank. *Nature* **342,** 533–537 (1989).
29. Davis, E. E. *et al.* An unequivocal case for high Nusselt-number hydrothermal convection in sediment-buried igneous oceanic crust. *Earth. Planet. Sci. Lett.* **146,** 137–150 (1997).
30. Matthews, M., Salisbury, M. & Hyndman, R. Basement logging on the Mid-Atlantic Ridge, Deep Sea Drilling Project Hole 3958. *Init. Rep. DSDP* **78B,** 717–730 (1984).

Acknowledgements

This work was supported by grants from the National Science Foundation and the United States Science Support Program to the Ocean Drilling Program. We thank C. Stein for suggestions, and P. Stauffer, J. Stein and E. Giambalvo for discussions that improved the manuscript.

Correspondence and requests for materials should be addressed to A.T.F. (e-mail: afisher@es.ucsc.edu).

A highly unsaturated fatty acid predicts carbon transfer between primary producers and consumers

Dörthe C. Müller-Navarra*, Michael T. Brett†, Anne M. Liston* & Charles R. Goldman*

** Department of Environmental Science and Policy, University of California, Davis, California 95616, USA*
† Department of Civil & Environmental Engineering, Box 352700, University of Washington, Seattle, Washington 98195,USA

The factors that regulate energy transfer between primary producers and consumers in aquatic ecosystems have been investigated for more than 50 years (refs 1–3). Among all levels of the food web (plants, herbivores, carnivores), the plant–animal interface is the most variable and least predictable link[4–6]. In hypereutrophic lakes, for example, biomass and energy transfer is often inhibited at the phytoplankton–zooplankton link[4], resulting in an accumulation of phytoplankton biomass instead of sustaining